Available online at www.sciencedirect.com
ScienceDirect
Journal of Volcanology and Geothermal Research 166 (2007) 125–146
Journal of volcanology and geothermal research
www.elsevier.com/locate/jvolgeores

Subsidence in the geothermal fields of the Taupo Volcanic Zone, New Zealand from 1996 to 2005 measured by InSAR

J.K. Hole [a,*], C.J. Bromley [b], N.F. Stevens [c], G. Wadge [a]

[a] *Environmental Systems Science Centre (ESSC), Harry Pitt Building, 3 Earley Gate, Whiteknights, University of Reading, Reading, RG6 6AL, UK*
[b] *GNS Science, Wairakei Research Centre, Private Bag 2000, Taupo, New Zealand*
[c] *GNS Science, PO Box 30368, Lower Hutt, New Zealand*

Received 28 September 2006; accepted 10 July 2007
Available online 11 August 2007

Abstract

A number of the geothermal systems in the Taupo Volcanic Zone (TVZ), New Zealand, have been utilised on a large scale to provide heat and to generate electricity, in some cases causing areas of localised subsidence. Subsidence monitoring using field-based surveys is practically constrained by limits to available resources so we have investigated the use of satellite differential radar interferometry (InSAR) for this purpose. Using ERS and Envisat radar data spanning 1996 to 2005, we have mapped the deformation at five of the heavily utilised geothermal fields of the TVZ. Subsidence signals were identified at the Ohaaki geothermal field from 1999–2004, and at Wairakei–Tauhara from 1996–2005, where our measurements compare well with coeval levelling data across the wider deformation field. Subsidence was also measured at Rotorua from 1996–2000. In favourable conditions, the InSAR measurements provide a relatively dense spatial coverage of the deformation field that extends well beyond the boundaries of the geothermal systems and beyond the scope of the networks of levelling benchmarks. In the case of the Wairakei–Tauhara geothermal field, using InSAR it is now possible to improve the spatial resolution near the field margins and to interpret the subsidence signals in the context of the wider, more regional, deformation. Our data also provide new insights into possible fault motion at the Mokai geothermal field occurring around the time of the commissioning of its first power station. We note, however, that the InSAR technique is not without limitations. High gradient subsidence features are poorly represented, although this can be resolved to some extent via a trade-off in data processing. Temporal decorrelation, a well known problem for this technique, is also an issue for TVZ geothermal fields. Therefore, we find that it is possible to provide fortuitous snapshots of the deformation at the TVZ geothermal fields, but operational monitoring using InSAR would be difficult as the proportion of suitable interferograms is low.

Keywords: New Zealand; Taupo Volcanic Zone; Subsidence; Geothermal fluid extraction

1. Introduction

The Taupo Volcanic Zone (TVZ) in New Zealand is an actively extending back-arc rift, developed in association with the subduction of the Pacific plate beneath the Australian plate. It is characterised by extensive volcanic and seismic activity (Wilson et al., 1995), which is accompanied by an exceptionally high heat output (~700 mWm^{-2}) channelled through twenty-three geothermal systems (Bibby et al., 1995).

Many commercial and domestic operations are permitted to extract small to medium quantities of

* Corresponding author.
E-mail address: jkh@mail.nerc-essc.ac.uk (J.K. Hole).

0377-0273/$ - see front matter © 2007 Elsevier B.V. All rights reserved.
doi:10.1016/j.jvolgeores.2007.07.013

water from a number of these geothermal systems and since the 1950s, some of the higher temperature fields (>220 °C) have been utilised on a larger scale to provide electricity (e.g. Carey, 2000). The reduction of subsurface pore pressure at some of these fields due to fluid extraction (without replacement) has affected the natural surface features and caused localised subsidence of up to 15 m (since 1950, at the centre of one bowl at Wairakei), which is more than in any other development involving fluid withdrawal (Allis, 2000). Measuring the spatial and temporal changes in the subsidence pattern can provide constraints on the permeability and compressibility properties of the compacting formations. These are important parameters for predicting future subsidence (Allis and Zhan, 2000). Monitoring of this subsidence in the TVZ is important to identify areas of infrastructure potentially at risk of structural damage and to reduce the impact of future development of the geothermal fields.

The extent and rate of subsidence at geothermal fields in the TVZ is currently measured by precise levelling across networks of benchmarks, repeated at intervals of one to five years (e.g. Allis, 2000). Changes in future development strategy, involving extraction and injection of fluids, may affect the size of the areas that will need to be monitored. Other field-based techniques, such as differential and continuous GPS, are also available and have been used in the TVZ to monitor deformation (e.g. Darby et al., 2000; Beavan and Haines, 2001), but the spatial density and repeat rate of field-based surveys are practically constrained by limits to available resources.

Differential Synthetic Aperture Radar Interferometry (InSAR) is a technique capable of measuring surface subsidence to centimetric precision over hundreds of square kilometres with a high spatial resolution (nominally ~25 m) (Massonnet and Feigl, 1998). Differential InSAR has been used successfully to measure deformation caused by geothermal fluid extraction, for example at East Mesa, California (Massonnet et al., 1997); Coso, Calfornia (Fialko and Simons, 2000; Vasco et al., 2002); and Cerro Prieto, Mexico (Carnec and Fabriol, 1999). It was also applied to two geothermal fields of the TVZ with mixed success (Hole et al., 2005b,c). This paper represents the first attempt to measure subsidence due to geothermal fluid extraction at all geothermal fields across the TVZ using InSAR. The study has two main objectives: firstly to assess the feasibility of using InSAR to measure the subsidence caused by geothermal development in the TVZ, and secondly to improve the ability to monitor future subsidence in this area.

2. Geological and hydrological setting

The TVZ covers an area of 40 km by 150 km (Fig. 1) and is defined by the envelope of active volcanism in the TVZ over the last two million years (Wilson et al., 1995). The TVZ is extending in an NW–SE direction at an average rate of 8 mm/year, north of Lake Taupo (Darby et al., 2000). The extension is not uniform in time or space. Geographically, it is divided into segments of active, largely normal, faulting in the central and western parts of the TVZ separated by non-extending "accommodation zones" (Rowland and Sibson, 2001). The volcanic activity is also segmented in nature: the central part is an area of extensive rhyolitic volcanism, producing over 10,000 km^3 of material from several large caldera systems; whereas andesitic volcanism predominates to the north–west and to the south. The depression left by regional tectonic subsidence and caldera collapse has been filled with rhyolite lavas and poorly- to non-welded ignimbrites interbedded with fluvial and lacustrine sediments, which in places is at least 2–3 km thick (Risk et al., 1999; Wood et al., 2001). Basement Mesozoic sandstones (graywacke), are found at the eastern and western margins of the TVZ but the composition of the crust beneath the Quaternary deposits in the TVZ itself is not fully understood (Stern et al., 2005).

A simplified representation of the structure and hydrology of the TVZ is given in Fig. 2. The hydrothermal convection is driven by a heat source at depth, the origin of which remains the subject of much debate (Hochstein, 1995). Conductive heat transport between the ductile base of the crust at 16 km (Stratford and Stern, 2004), and the bottom of the brittle convective region at 8 km (Bibby et al., 1995) can only supply 60% of the observed heat flow at the surface, so heat must reach the convective zone by other mechanisms such as repeated intrusion from the mantle (Bibby et al., 1995). Stress redistribution associated with such intrusions of ductile material at depth could lead to large temporal and spatial variations in surface deformation rates.

Within the shallow (0–3 km) volcanic-sedimentary sequences, the highly permeable layers (aquifers) act as geothermal fluid reservoirs (containing liquid or vapour), and have interlayers of poorly permeable rocks (aquitards). The water heated at depth forms narrow convective plumes which rise and spread laterally into the shallower aquifers. The hot fluids may boil and escape to the surface as water or steam via permeable paths though the aquitards provided by faults and fractures (e.g. Soengkono, 1999, 2000). Through boreholes, fluids may also be discharged as steam-brine

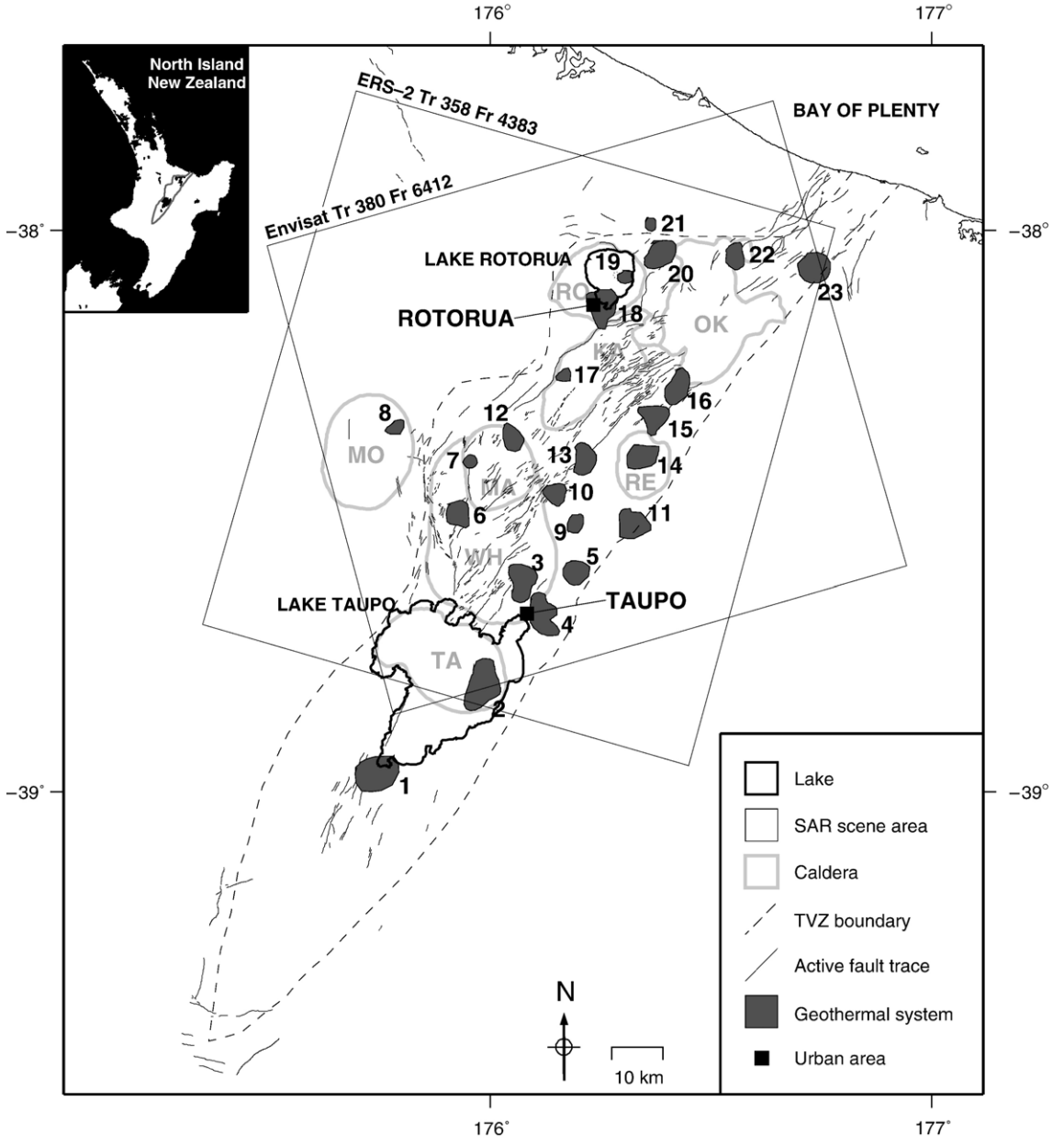

Fig. 1. Location map showing the geothermal fields in the TVZ (from Bibby et al., 1995), 1—Tokaanu, 2—Lake Taupo, 3—Wairakei, 4—Tauhara, 5—Rotokawa, 6—Mokai, 7—Ongaroto, 8—Mangakino, 9—Ngatamariki, 10—Orakeikorako, 11—Ohaaki, 12—Atia-muri, 13—Te Kopia, 14—Reporoa, 15—Waiotapu/Waikite, 16—Waimangu, 17—Horohoro, 18—Rotorua, 19—East Rotorua, 20—Tikitere/Rotoiti 21—Taheke 22—Rotoma/Tikorangi, 23—Kawerau. The locations of the calderas and the TVZ boundary are after Wilson et al. (1995), TA—Taupo, Mo—Mangakino, WH—Whakamaru, MA—Maroa, KA—Kapenga, RO—Rotorua, RE—Reporoa, OK—Okataina. The current active fault locations are from the New Zealand Active Faults database (GeoNET, 2006a). The average footprints of the SAR images used in this study are shown.

mixtures or re-injected as cooler brine-condensate mixtures. The geothermal systems are naturally recharged by the downward flow of cold meteoric water across the TVZ, and by degassing magmatic brines.

The horizontal extent of the geothermal systems can be defined by abrupt changes in electrical resistivity (Bibby et al., 1995, and references therein). The extent and distribution of the 23 active systems identified within the central TVZ and other important geological

features are shown in Fig. 1. It has been shown that locations of the geothermal systems appear to have remained remarkably stable over the last 200 Ka and that the locations of some of the systems can be related to the TVZ structure (Rowland and Sibson, 2004; Kissling and Weir, 2005). There is a notable absence of geothermal systems in the heavily rifted and seismically active central and western parts of the TVZ (Bibby et al., 1995), which are thought to be areas of recharge.

3. Effects of geothermal development

Table 1 gives details of the six geothermal systems (of the twenty three in total in the TVZ) that have been exploited on a large scale for electricity production or process heat and the effects of development. There have been no large-scale electricity generation projects at Rotorua, but it is included in this study because the shallow aquifer (<300 m), has been extensively utilised to provide domestic heating and hot water bathing.

Fluid extraction from wells drilled into the aquifer in some cases has caused a decrease in subsurface pore pressure, which has affected the natural surface geothermal features. The outflows of famous geysers and springs at Rotorua were initially adversely affected by withdrawal from shallow wells in the 1960s (Turner, 1985; Allis and Lumb, 1992), but since 1987 these features have largely recovered in response to field-wide pressure increases, achieved by controlling extraction and increasing reinjection (Scott and Cody, 2000). Since the 1990s, discharges have recommenced at a number of vents in built up areas, that were filled in after the decline and disappearance of thermal features (Scott et al., 2005). At Wairakei and Tauhara, the deep saline waters that once fed geysers and mineralised hot springs were lost as a result of deep pressure drawdown of 25 bar from steam and water extraction between the 1950s and 1970s. Since 1980, deep liquid pressures have stabilised as a result of increased natural recharge induced by the initial pressure drop. Another effect of initial pressure drawdown at Wairakei was an increase in subsurface boiling and a consequent increase in steam-heated surface features such as fumaroles, hot ground, thermally-tolerant vegetation, steam-heated springs and a few hydrothermal eruptions. The presence of pressurised shallow steam zones fed by boiling deep aquifers

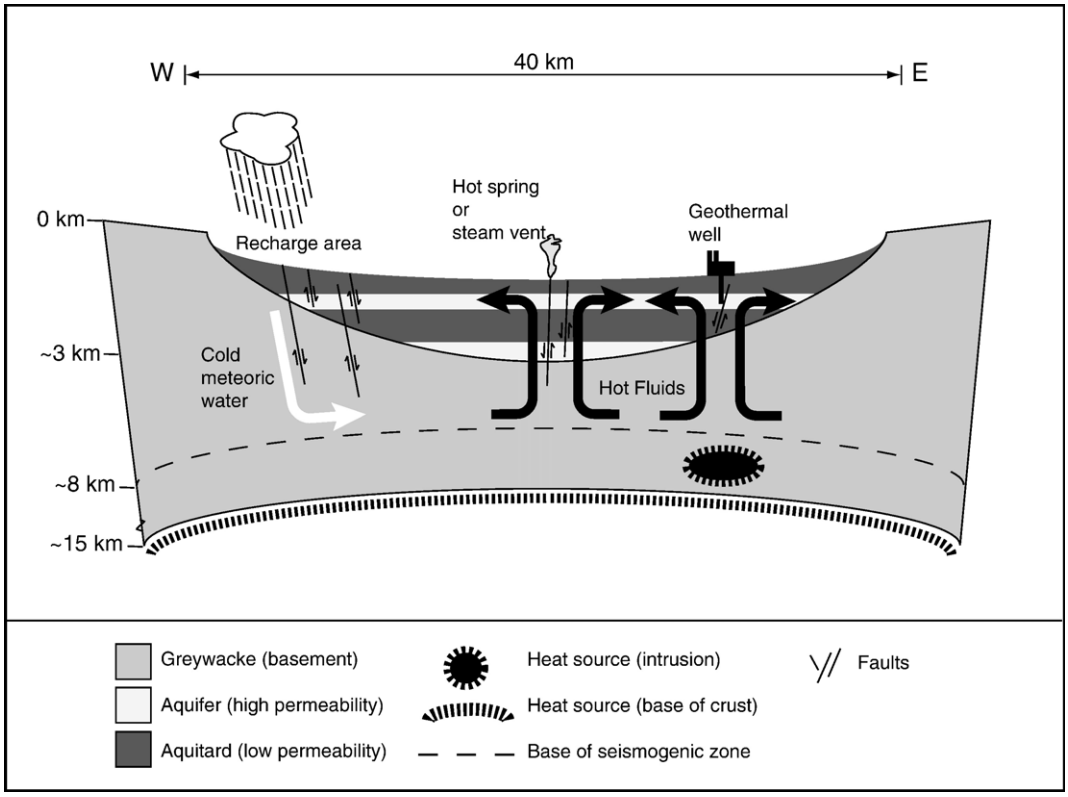

Fig. 2. Schematic of the structure and hydrology of the TVZ showing the heat source at the base of the crust and possible intrusions.

Table 1
Summary of major developments at the geothermal fields in the TVZ (modified after Dunstall, 2005) and the effects of development

Geothermal field	Power plant	Year of commissioning	Capacity (MW)[a]	Known exploitation effects	InSAR detected deformation
Ohaaki	Ohaaki	1989	104	Subsidence, loss of natural features (Allis et al., 1997a,b; Glover et al., 2000)	Subsidence
Wairakei–Tauhara	Wairakei	1958	165	Subsidence, loss of natural features (Allis, 2000)	Subsidence, inflation
	Poihipi Road	1996	55		
Mokai	Mokai I	1999	57	Subsidence (Energy Surveys Ltd, 2003)	Inflation
	Mokai II	2005	39		
Rotokawa	Rotokawa	1997	31	No deformation (Energy Surveys Ltd, 2002)	Possible subsidence
Kawerau	Kawerau Binary	1990	6.5	Subsidence, loss of natural features (Allis, 1997)	–
	Tasman P&P Co	1966	40[b]		
Rotorua	–	1920s[c]	–	Loss and restoration of natural features (Scott et al., 2005)	Possible subsidence

[a] Total installed capacity.
[b] Equivalent including direct use of steam for the paper mill.
[c] Approximate start of exploitation.

complicates the relationship between the fluid extraction or injection activities and the pressure-related surface effects observed such as changes to discharging features and subsidence.

A reduction in pressure can also cause compaction of an aquifer or adjacent aquitard due to loss of support and compression of the skeleton of the porous formation (Helm, 1984), leading to subsidence at the surface. Extraction related subsidence is known to have occurred at the Ohaaki, Wairakei–Tauhara, Kawerau and Mokai geothermal fields (see Table 1). Subsidence at Wairakei–Tauhara and Ohaaki is thought to be due to the subsurface compaction of the relatively compressible, low permeability Huka Falls Foundation (HFF) mudstone aquitards between 50 and 300 m depth (Allis, 2000). The subsidence is not uniform across the area of reduced pressure, or the area within the resistivity boundary, but forms localised bowls. This is most likely because the effective compressibility varies laterally within the upper HFF mudstone unit and is much greater beneath the subsidence bowl than in the remainder of the field (Allis, 2000). Slow propagation of pressure decline into the aquitard causes a delay in the subsidence response. Another delaying process that may be significant is inelastic deformation, or creep (Bromley, 2006). This is particularly relevant for high-porosity formations containing a high percentage of hydrothermal clays. At Wairakei–Tauhara and Ohaaki the subsidence still continues, although at gradually falling rates, probably due to the slow drainage of the HFF mudstone layer (Allis, 2000).

In principle, the pore pressure can be maintained by re-injection of water but this is not always achievable due to the possibility of cool re-injection water returning too rapidly and prematurely cooling the production aquifer. Full re-injection is practised at Mokai and Rotokawa, and to a limited extent at Wairakei–Tauhara, Ohaaki and Kawerau.

4. InSAR processing

4.1. Method

A detailed description of the use of InSAR to study ground deformation can be found in Massonnet and Feigl (1998) but some key points are noted here. Two synthetic aperture radar (SAR) images are obtained by the satellite at different times from a similar position along repeated orbital passes. Complex multiplication of the aligned pixels of the two SAR acquisitions produces an interferogram, from which the difference in the radar path length between the acquisitions, termed the phase shift, ϕ, is obtained.

Certain conditions are required for a coherent InSAR signal. The surface scattering energy must remain relatively unchanged between acquisitions, or decorrelation will occur. Success depends on the geometric configuration of the satellite between subsequent passes, parameterised by the perpendicular baseline, $B_\perp$ (the distance between imaging positions perpendicular to the look direction of the radar) and also the temporal separation between SAR acquisitions. Both affect the

degree of coherence of the interferogram, γ (Zebker and Villasenor, 1992). Larger values of $B_\perp$ (several hundred metres depending on surface relief) and greater intervals between images tend to reduce the quality of the phase. The measured interferometric phase is given by Eq. (1):

$$\phi = \phi_{\text{def}} + \phi_{\text{ref}} + \phi_{\text{top}} + \phi_{\text{atm}} + \phi_{\text{n}} \quad (1)$$

where,

$$\phi_{\text{def}} = \frac{4\pi}{\lambda} D \quad (2)$$

$$\phi_{\text{ref}} = \frac{4\pi}{\lambda} B_{||} \quad (3)$$

$$\phi_{\text{top}} = \frac{4\pi}{\lambda} \frac{B_\perp H}{R_1 \sin\theta} \quad (4)$$

ϕ_{def} is the component of the phase due to surface displacement, D, in the direction of the satellite (Eq. (2)). λ is the SAR wavelength. The reference phase, ϕ_{ref}, is the expected phase shift due a reference surface derived from the shift in the orbital trajectory between the two image acquisitions (Eq. (3)). $B_{||}$ is the parallel baseline (the distance between imaging positions parallel to the look direction of the radar). ϕ_{top} is the contribution of the phase from the topography (Eq. (4)), where H is the height above the reference surface, R_1 is the radar range and è is the look angle of the radar. ϕ_{atm} is the contribution to the phase from the delay due to atmospheric water vapour, and φ_{n} represents the phase noise innate to the instrumentation.

An accurate digital elevation model (DEM) is used to remove the contribution to the interferograms from the topography (ϕ_{top}). We used a DEM produced by digitizing and interpolating between 25 m interval contours from the national 1:50,000 topographic map series produced by Land Information New Zealand (LINZ) (e.g. Land Information New Zealand, 1987). The estimated vertical accuracy of the DEM is 10 m (Barringer and Lilburne, 1997), and as the magnitude of ϕ_{top} is proportional to $B_\perp$, to minimise the impact of any errors in the DEM a maximum perpendicular baseline threshold of 300 m was applied in data selection.

ϕ_{n} was reduced by adaptive filtering using the technique of Goldstein and Werner (1998) with a filter window of 2 and a filter parameter of 1.0, following complex multi-looking by a factor of 4 pixels in range and 16 in azimuth (Massonnet and Feigl, 1998) to reduce the phase noise. As a result, the maximum theoretical detectable deformation gradient (Massonnet et al., 1996) is 0.35 mm/m for a pixel size of 80 × 65 m.

Errors in the estimation of ϕ_{ref} are reduced by using precise orbit estimates (Closa, 1998). Any residual errors in ϕ_{ref} can be estimated and modelled as a plane across the interferogram (Hanssen, 2001) but a high level of coherence is required in order to identify a phase ramp and estimate the parameters of the plane. This was only possible for a small number of interferograms, but as the

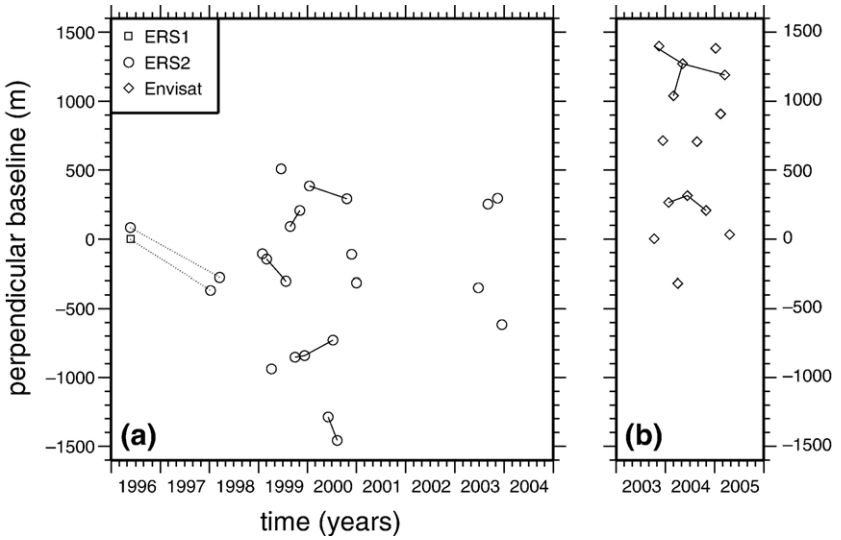

Fig. 3. Perpendicular baselines for (a) ERS, track 358, frame 4383, referenced to ERS-1 orbit 25396 and (b) Envisat, track 380, frame 6412, referenced to orbit 08542. Pairs of images referred to in this study are connected by solid lines. The dotted line shows long period interferograms used in the urban area of Rotorua.

geothermal systems are small compared to the swath width of the interferograms, this is unlikely to have a large effect on the subsidence measurements.

The interferogram phase information is in modulo 2π format (a wrapped interferogram), and so in order to obtain D, the interferograms must be unwrapped. This requires a high level of coherence that cannot be met for all interferograms. The unwrapping has been carried out using the minimum L^p-NORM method as implemented by Ghiglia and Pritt (1998). In order to assist the unwrapping a phase quality mask was used, calculated from the phase variance of the interferogram.

The atmospheric contribution ϕ_{atm} is not correlated with time, so can be reduced by combining multiple interferograms, a technique known as stacking. This has been carried out using two methods. The first method involves averaging of interferograms which do not share common images (i.e. they are independent). This reduces the errors arising from these contributions by $\frac{1}{\sqrt{N}}$, where N is the number of interferograms. The deformation rate is assumed to be linear in time. No weighting is required if the interferograms have an equal (or very similar) temporal separation. If the time periods of the interferograms are different, then any weighting applied will give a disproportionate weight to any atmospheric noise contributions from the short period interferograms. The second method involves the linear integer combination of interferograms (Hanssen, 2001). The atmospheric delay from images other than the first and last image in the stack is cancelled. Using this method, unwrapping only need be carried out after stacking; however, the overall temporal separation must be small enough so that it is still possible to sample any large deformation gradients. Both stacking methods cause a loss of data in areas which do not retain coherence in all of the contributing interferograms.

Lastly, D represents the one-dimensional motion towards the radar. If the assumption is made that the subsidence occurs only in the vertical direction then this can be retrieved by the multiplication of D by $(\cos\theta)^{-1}$ (Hanssen, 2001).

4.2. Data

Radar data acquired by the ERS-1, ERS-2, and Envisat satellites were used in this study. The ERS-1/2 scene that covers the maximum area of the TVZ region (Fig. 1) was acquired on the satellite's descending-pass (track 358, frame 4383) for which there are 24 images available in the archive from 1996 to 2003. Ascending-pass ERS data have not been considered because the archived dataset is too small. The paucity of data are partly due to a lack of an operational local receiving station prior to 1995, and also because the satellite had not been commissioned to acquire images of the area (e.g. Stevens and Wadge, 2004). ERS-1 stopped acquiring data in 1999, and due to technical difficulties with the ERS-2 satellite, no acquisitions of the TVZ have been commissioned since 2003.

Since the launch of Envisat in 2003, ascending-pass Envisat data have been commissioned and acquired mostly every 35 days, at a look angle of 23° from the vertical. Fourteen ASAR images (track 380, frame 6412, see Fig. 1) were available for this study from October 2003 to April 2005. Fig. 3 shows the distribution of perpendicular baselines for image pairs with time for the ERS and Envisat data used in this study.

Both the ERS and Envisat scenes cover all the geothermal fields in the TVZ that are undergoing exploitation except the Kawerau geothermal field, which falls just outside the ERS scene and is only partially covered, to differing extents, by the Envisat ascending-pass scenes.

5. Results and discussion

5.1. Coverage of the geothermal fields

Weathering, vegetation and man-made changes all affect the scattering characteristics of the land surface, leading to a loss of coherence (termed temporal decorrelation)(Zebker and Villasenor, 1992). The land cover in the TVZ is mainly forest and farmland, which have a variable coherence that depends on the temporal and perpendicular baselines, weather conditions and season. Undisturbed indigenous forest rarely retains coherence between successive 35 day passes, or even over one day, as we have observed elsewhere in New Zealand in ERS-1/ERS-2 tandem pairs. Conversely, the commercially managed forests, which are mostly coniferous monocultures in different stages of growth, do maintain some areas of coherence — recently harvested areas, or areas with young trees and low canopy cover, are less affected by temporal decorrelation.

The Rotorua geothermal field lies largely within the urban area of Rotorua, and the western part of the Tauhara geothermal field underlies part of Taupo Town. The remaining part of the Tauhara field, the Mokai, Wairakei, Rotokawa and Ohaaki fields and the other geothermal systems shown in Fig. 1 all fall within vegetated areas. Only a small number of interferograms, with time periods of less than six to eight months and with low perpendicular baselines, were identified as having adequate coherence to recover the deformation

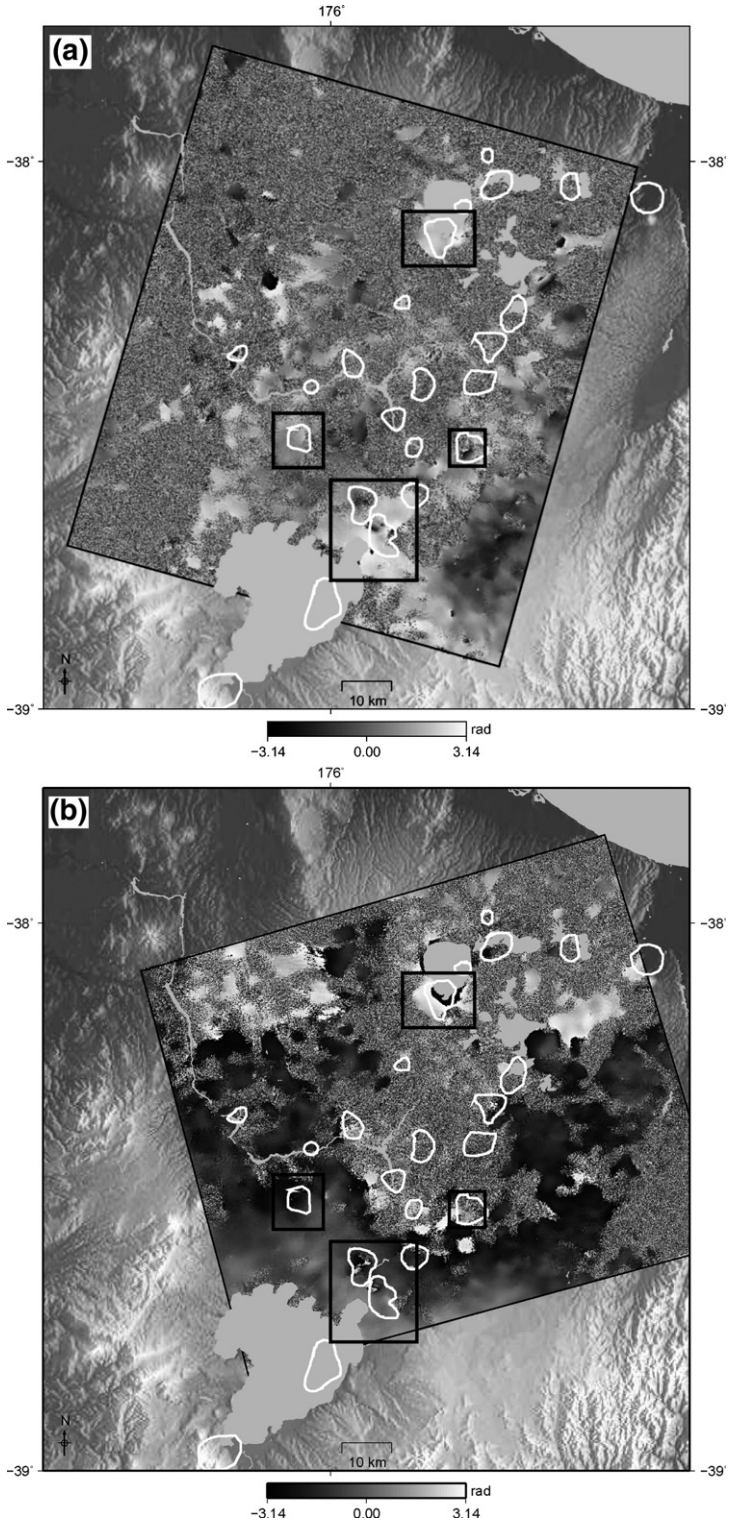

Fig. 4. Wrapped interferograms overlaid on a shaded relief image: (a) ERS 05/03/1999–23/07/1999, (b) Envisat 13/06/2004–31/10/2004. Also shown are the outlines of the lakes (grey) and the geothermal fields (white) (from Bibby et al., 1995). White, grey to black represents increased distance to the satellite (i.e. apparent subsidence). The locations of the Wairakei–Tauhara, Mokai, Ohaaki and Rotorua study areas are outlined in black.

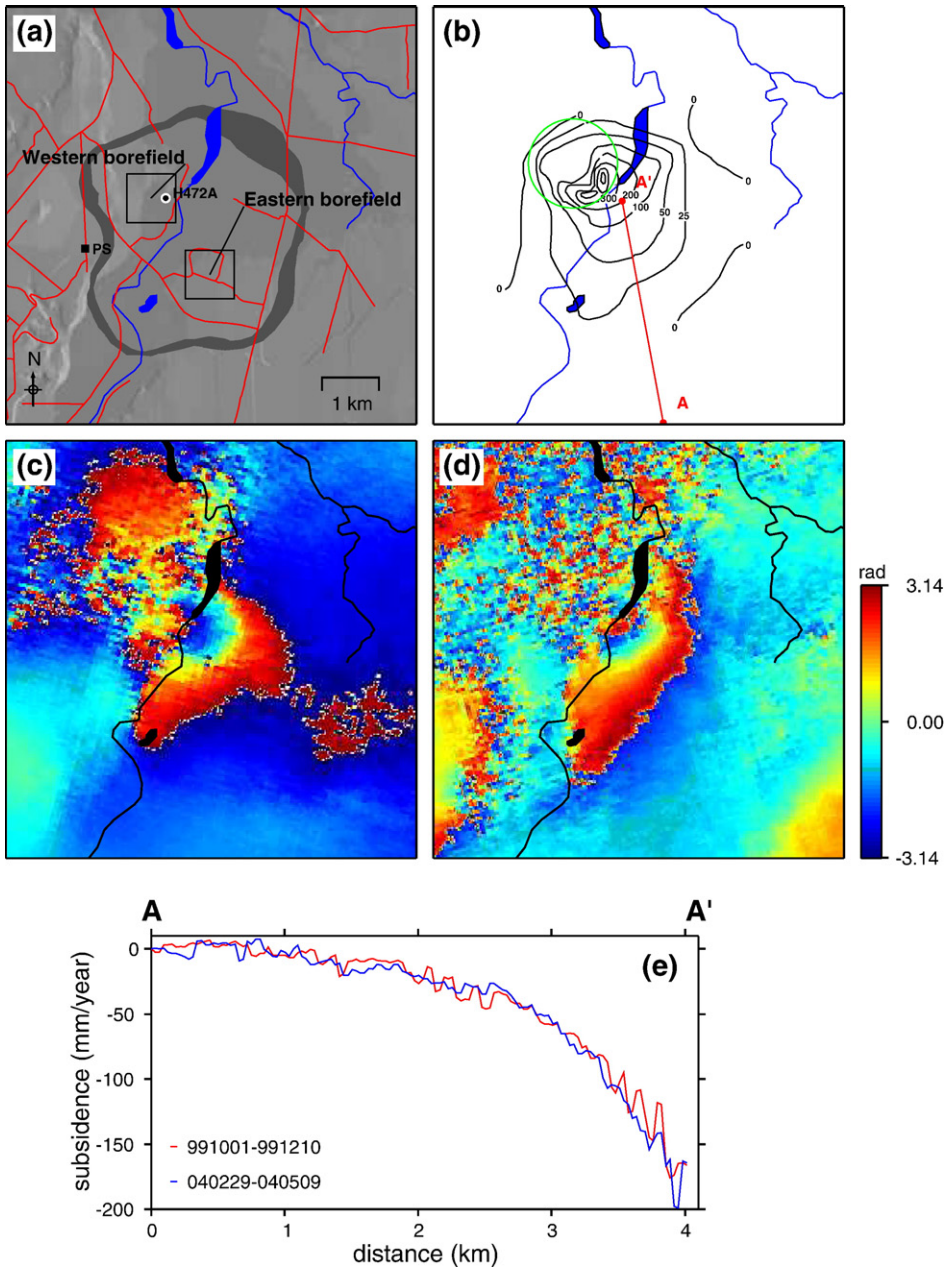

Fig. 5. (a) Location map of the Ohaaki geothermal field showing lakes and rivers (blue), road outlines (red), resistivity boundary (grey) (after Bibby et al., 1995, Fig. 14), the locations of the power station (PS) and selected benchmarks discussed in the text. The green circle marks the approximate location of the buried Ohaaki rhyolite NE dome (Allis et al., 1997a). (b) Vertical displacement rate (in mm/year) obtained from levelling for the 2/1993 to 1/1995 period (after Allis et al., 1997a). Wrapped interferograms of the Ohaaki geothermal field (c)–(d): (c) ERS, 01/10/1999–10/12/1999, (d) Envisat, 29/02/2004–09/05/2004. Red, yellow to blue represents increased distance to the satellite (i.e. apparent subsidence). (e) Profile from A to A′ of the deformation rate in mm/year relative to A, estimated from the unwrapping of ERS interferograms 01/10/1999–10/12/1999 in (a) and Envisat interferogram 29/02/2004–09/05/2004 (b).

in these non-urban areas. For example, Fig. 4 shows two wrapped interferograms with a perpendicular baseline of less than 100 m and a time period of less than six months. In both of these examples some of the geothermal areas are more coherent than others, and the general pattern is that those in the central TVZ are

generally less coherent, whereas those further south near Lake Taupo are more coherent.

Interferograms with longer time periods are largely decorrelated outside of the urban areas. Hence, the uneven temporal distribution of the ERS data (see Fig. 3) means that the deformation (in non-urban areas) cannot be measured from 1996 to 1998, and from 2001 to 2003. The interferograms used in this study are shown in Fig. 3.

5.2. Deformation signals

In Fig. 4 much of the spatial variance of the signals is uncorrelated atmospheric signal, but consistent, localised, deformation signals are identifiable within the boundaries of the Ohaaki, Wairakei, Tauhara, Mokai and Rotorua geothermal systems (as located in Fig. 4). These will now be discussed in more detail. The Rotokawa geothermal system has been undergoing geothermal development since 1997 and the InSAR measurements suggest a very weak subsidence signal. However, the results are inconclusive and we will therefore not discuss this field in depth. As we mentioned previously, deformation at Kawerau could not be observed because it lies beyond the spatial extent of our ERS and Envisat data (Fig. 1).

5.2.1. Ohaaki

The resistivity boundary of the Ohaaki geothermal field is shown in Fig. 5a. Since production began in 1988 a maximum subsidence of 3.3 m has been measured using levelling (as of 2002) (Central Surveys Ltd, 2002). Vertical displacement rate contours derived from interpolation of levelling data from 1993 to 1995 are shown in Fig. 5b (Allis et al., 1997b). It should be noted that this levelling-derived subsidence map predates the period of the InSAR. The subsidence bowl is situated over the eastern flanks of the buried Ohaaki Rhyolite NE dome. The HFF overburden is thinnest at the crest of the dome, which is responsible for the kidney shape of the subsidence bowl (Allis et al., 1997a). At Ohaaki, as much as practicable (with a condensing type turbine) of the available discharged

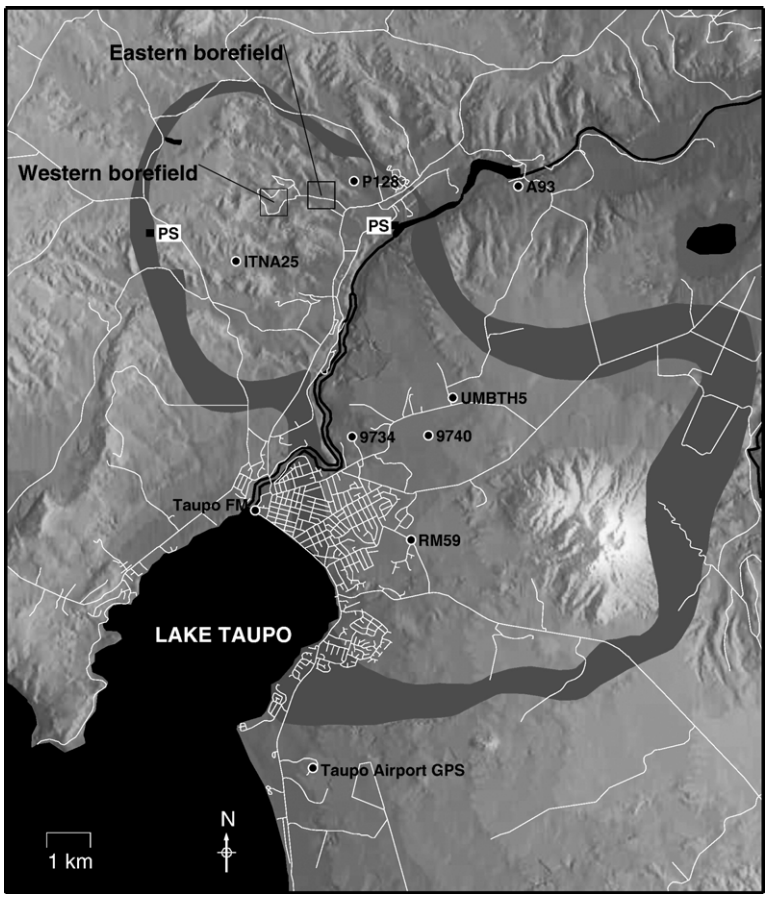

Fig. 6. Location map of Wairakei–Tauhara geothermal field showing lakes and rivers (black), road outlines (white), resistivity boundary (grey) (after Bromley et al., 2000), the locations of the power stations (PS) and selected benchmarks discussed in the text.

fluids is re-injected. This ranged from about 86% (1989–1994) to 76% (2004) (decreasing with time because of rising discharge enthalpy and more steam loss through the evaporative cooling tower).

Seven interferograms were found to have adequately coherent data to measure most of the deformation field, six from ERS and one from Envisat. These mostly have time periods of 70-days or less (e.g. Fig. 5c and d). Generally, the coherence is higher on the eastern side of the Waikato River. The area west of the river is predominantly forested and is more affected by temporal decorrelation. Interferograms with time periods greater that 70-days generally have a low coherence in the Ohaaki area and are all completely decorrelated in the area around the centre of the bowl. It is possible that this observed decorrelation may be caused by the increasing subsidence towards the centre of the bowl. Tilt values around the Ohaaki bowl range from 0.7 to 2.3 mm/m/year (from 1998–2002). In a 70-day period the tilt could be as much as 0.44 mm/m, which is beyond the maximum detection capability of C-band InSAR (0.35 mm/m for the pixel size of 80 × 65 m used in our processing). As the level of decorrelation increases, the maximum detectable deformation gradient decreases as it becomes more difficult to define the fringes (Baran et al., 2005).

The Ohaaki subsidence bowl is evident in both Fig. 5c and d. Comparing these interferograms with the levelling data suggests that the location and extent of the subsidence bowl has not changed significantly from 1993 to 2004. Fig. 5c shows that in 1999, the subsidence was greatest in the north-western part of the field, coincident with the Western borefield, in the same location as the centre of the deformation in Fig. 5b.

The maximum rate of subsidence (near benchmark H472A) measured by levelling from 1993 to 1995 was 450 mm/year, declining to less than 300 mm/year from 1995 to 1998 (Allis and Zhan, 2000). The 70-day interferograms in Fig. 5c and d were unwrapped and scaled to estimate the deformation rates at Ohaaki from October to December 1999 and from February to May 2004 (±6 mm/year). The deformation field is most clearly defined on the eastern side of the Waikato river. It is not possible to measure the largest deformation gradients that occur in the centre of the subsidence bowl, as unwrapping was not possible due to decorrelation. A profile was taken across both interferograms from a point away from the geothermal field, point A, to point A′ near the Waikato river (Fig. 5e). A comparison of the two profiles shows that the deformation rate towards the margins of the subsidence bowl has not changed significantly between 1999 and 2004. The deformation rate (at least 160 mm/year at A′) appears to have fallen since the 1993 to 1995 levelling survey.

5.2.2. Wairakei–Tauhara

The Wairakei and Tauhara geothermal fields are hydrologically linked and the resistivity boundary of the combined system (Wairakei to the north-west and

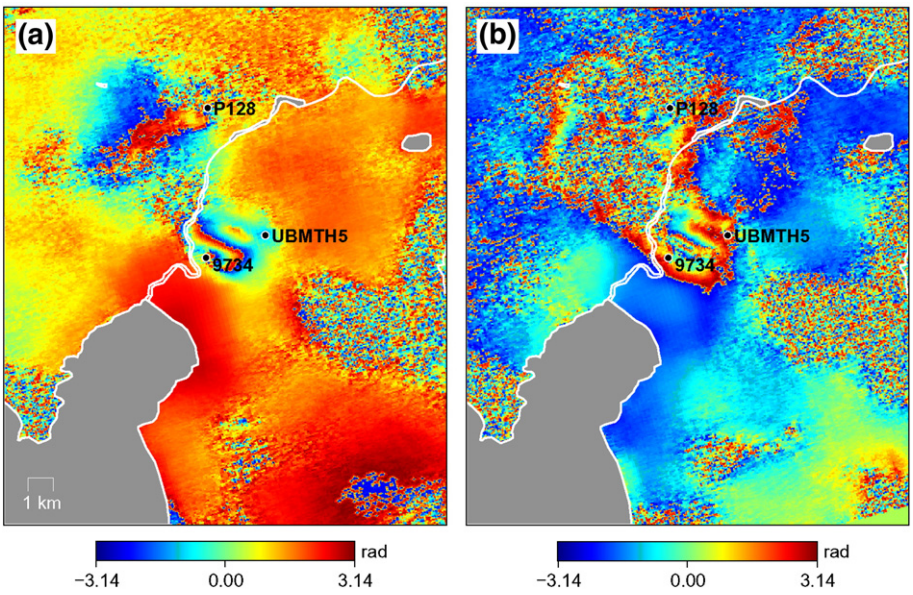

Fig. 7. Wrapped Envisat stacked interferograms of the Wairakei–Tauhara geothermal field: (a) 12/10/2003–09/05/2004–20/03/2005, (b) 25/01/2004–13/06/2004–31/10/2004. Red, yellow to blue represents increased distance to the satellite (i.e. apparent subsidence).

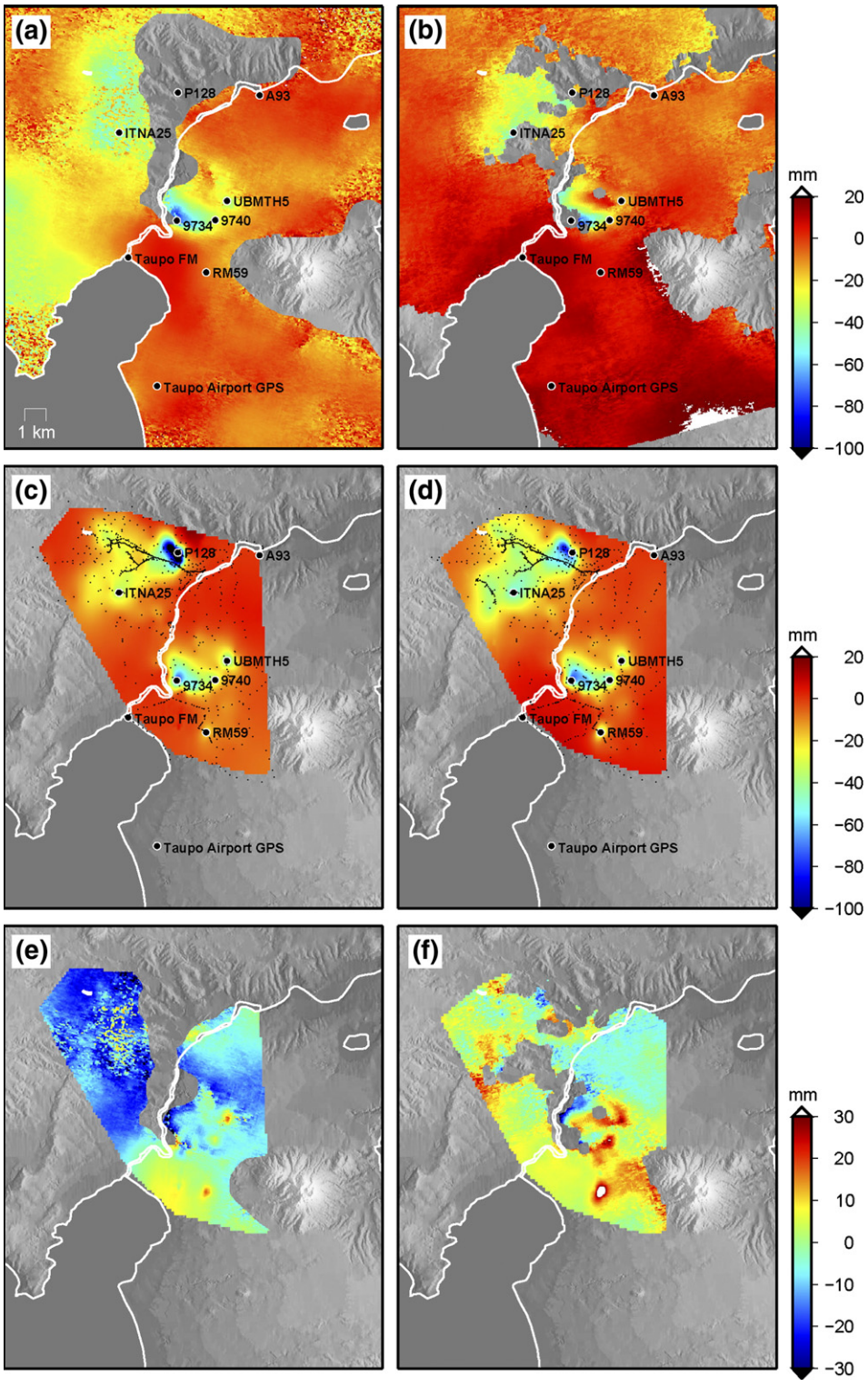

Fig. 8. Unwrapped interferograms of the Wairakei Tauhara geothermal field showing line-of-sight displacement in mm/year: (a) ERS stack of four interferograms 01/10/1999–10/12/1999, 05/03/1999–23/07/1999, 27/08/1999–05/11/1999 and 02/06/2000–11/08/2000, (b) Envisat interferogram 13/06/2004–31/10/2004. Vertical displacement rates (in mm/year) obtained from levelling (after Energy Surveys Ltd, 2005): (c) 06/1997 to 03/2001, (d) 03/2001 to 12/2004. The locations of levelling benchmarks used in the interpolation are shown. (e) Residual of (a)–(c). (f) Residual of (b)–(d).

Tauhara to the south-east) is shown in Fig. 6. Fluid extraction has been occurring since the 1950s from the Wairakei field from two main areas, marked as the Eastern and Western borefields. Partial re-injection (about 25–30% of available fluids) commenced in 1997 near the power station on the Waikato river (PS in Fig. 6).

As at Ohaaki, the subsidence history of the Wairakei and Tauhara fields has been well monitored by levelling and total subsidence of up to 15 m (between 1950 and 2004) is inferred to have accumulated at the centre of the main bowl about 500 m east of the Wairakei Eastern borefield, near where a lake has formed in the Wairakei Stream valley. Field-wide levelling surveys have been carried out in 1997, 2001 and 2004, with smaller local surveys in between.

Outside the urban areas, the majority of the Wairakei–Tauhara field is farm or grassland. There are a number of forested areas within the Wairakei geothermal field that have a detrimental effect on the temporal decorrelation. Hole et al. (2005b) already showed that interferograms with a 70-day temporal separation have a high coherence across the Wairakei–Tauhara geothermal area, although the deformation signal across the wider field is below the minimum detection capability of C-band InSAR. Hole et al. (2005b) also found a coherent deformation signal in interferograms with a temporal separation of up to three years from 1996 to 2003, but only in the urban area of Taupo.

In the present study, one ERS and five Envisat interferograms with intervals longer than 70 days were identified as having a high enough level of coherence over the Wairakei–Tauhara geothermal area to map the detailed spatial pattern of deformation. Four of the Envisat interferograms were combined in two independent linear stacks. The first stack, Fig. 7a, spans 0.77 years from January 2004 to October 2004 and the second a longer interval of 1.44 years from November 2003 to March 2005 (Fig. 7b). Both images show a

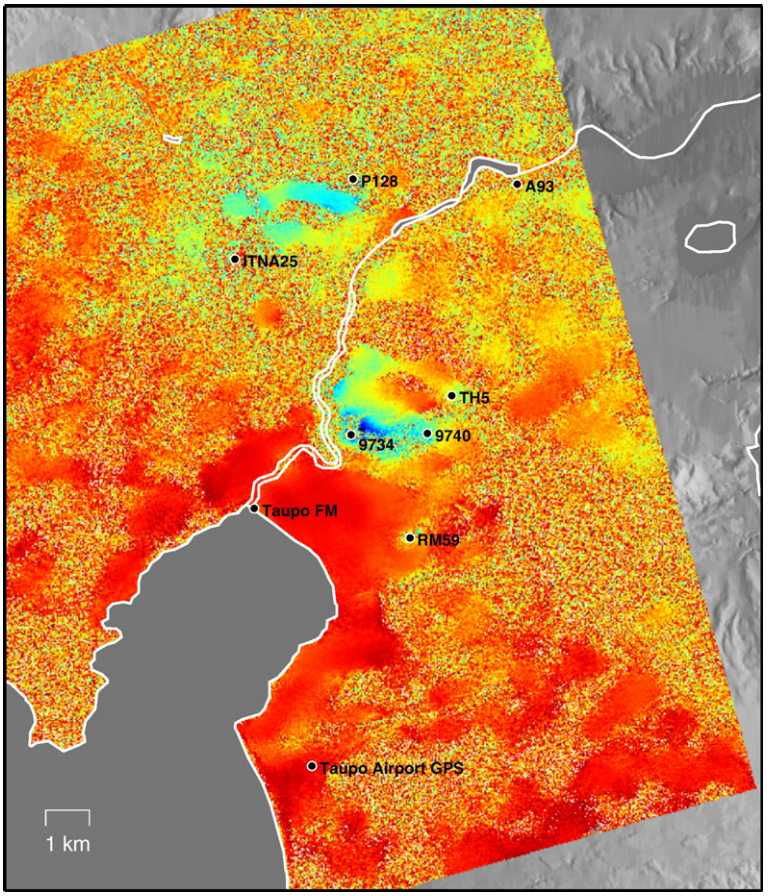

Fig. 9. Unwrapped Envisat interferogram 13/06/2004–31/10/2004 of the Wairakei–Tauhara geothermal field, showing line-of-sight displacement in mm/year with 1 × 4 looks.

Table 2
Deformation in mm/year of Taupo Fundamental (Taupo FM) benchmark relative to benchmark A93

Levelling (mm/yr)		InSAR (mm/yr)	
Period	Taupo FM	Period	Taupo FM
06/1997–03/2001	−1	05/03/1999–11/08/2000	−5
03/2001–12/2004	+8	13/06/2004–31/10/2004	+11

similar distribution and extent of subsidence but Fig. 7b shows a loss of coherence in some parts of the field due to temporal decorrelation and high spatial phase gradients. Both images show that some subsidence is occurring across almost the entire area of the Wairakei geothermal field, continuing into the northwestern part of the Tauhara field. Three main areas of significant subsidence are evident from Fig. 7. The first is the well-known Wairakei subsidence bowl, although the area of maximum subsidence in the centre of the bowl (near benchmark P128), is not resolved due to incoherent data in that area. There are also two smaller subsidence bowls on the south side of the Waikato river in the north of the Tauhara field, the first centred on Spa Park (benchmark 9734) and a second smaller area on Rakaunui Road (benchmark UBMTH5). These compare well with levelling data.

Fig. 7a and to a lesser extent, Fig. 7b show that there may be a weak subsidence signal spanning the north-western boundary of the Rotokawa geothermal field (top-right of the images). However, this area is heavily affected by decorrelation and the subsidence signal is not present in many of the shorter-term coherent interferograms. We are therefore not able to comment further on the origin of this apparent signal and whether or not it is related to the geothermal field. The results of levelling surveys suggest that little or no deformation has occurred at Rotokawa (Energy Surveys Ltd, 2002).

The annual deformation rate estimated from a stack of three 70-day and one 140-day unwrapped ERS interferograms from March 1999 to August 2000 is shown in Fig. 8a. Fig. 8b shows the deformation rate estimated from a 140-day Envisat interferogram from June to October 2004. The deformation was scaled to mm/year relative to benchmark A93 at Aratiata Dam and areas of low coherence and areas where unwrapping was not possible have been masked out.

Interpolated vertical displacement rate contours were also derived from the 1997 to 2001 and 2001 to 2004 levelling data, relative to benchmark A93, and are shown in Fig. 8c and d (Energy Surveys Ltd, 2005). On comparing the levelling surveys with the interferograms, we found that there is generally a good agreement in the subsidence pattern between the InSAR and the levelling. However, there were a number of areas where the InSAR data provide coverage where there is no levelling data or the density of levelling benchmarks is relatively low. This is most evident in the south-western part of the Wairakei field, particularly around benchmark ITNA25, where subsidence rates have increased from 36 mm/year, from 1997 to 2001, to 52 mm/year from 2001 to 2004. The full extent of this subsidence feature is difficult to resolve using the current levelling network. Conversely, there are also areas where our InSAR stacks do not detect deformation observed during the levelling surveys, and we will discuss this next.

Fig. 8e and f are images of the residual differences between the InSAR and levelling deformation rates from 1997 to 2001 and 2001 to 2004 respectively. The levelling data show a small subsidence bowl centred on the junction with Crown Road and Invergarry Road (benchmark RM59) that began to develop in 1997 (Bromley and Currie, 2003) and another apparent subsidence feature centred on benchmark 9740 near Centennial Drive, as discussed by White (2005). The RM59 feature is not resolved in the InSAR images and the 9740 feature appears to be an extension of the Spa Park (9734) feature.

Maximum tilt rates measured between 2001 and 2004 at Spa Park and Crown Road are between 0.46 and 0.56 mm/m/year, occurring across narrow (~50 m wide) regions around the bowl edges. In a 140-day period, the tilt values are approaching the limit of the maximum resolvable deformation gradient for a pixel size of 80×65 m (0.35 mm/m). Reducing the averaging window to 1×4, produces pixel dimensions of 20×16 m, and increases the maximum detectable deformation gradient to 1.4 mm/m.

Fig. 9 shows a 140-day Envisat unwrapped interferogram from June 2004 to October 2004 where the averaging window has been decreased to 1×4 (20×16 m). The non-coherent areas have not been masked. Although there is some coherence loss, higher deformation rates can be measured in the Spa Park area (near benchmark 9374). This shows a good agreement with the levelling at about 88 mm/year. Fig. 9 also shows the localised subsidence at Crown Road, centred near benchmark RM59, which was not previously identifiable. It is clear that reducing the averaging allows the higher deformation gradients to be resolved giving a better representation of the deformation field but at the expense of wider coverage.

Fig. 8b shows that in 2004 there was an apparent uplift of Taupo Town relative to benchmark A93, about 10 km to the north-east. This uplift continues to the

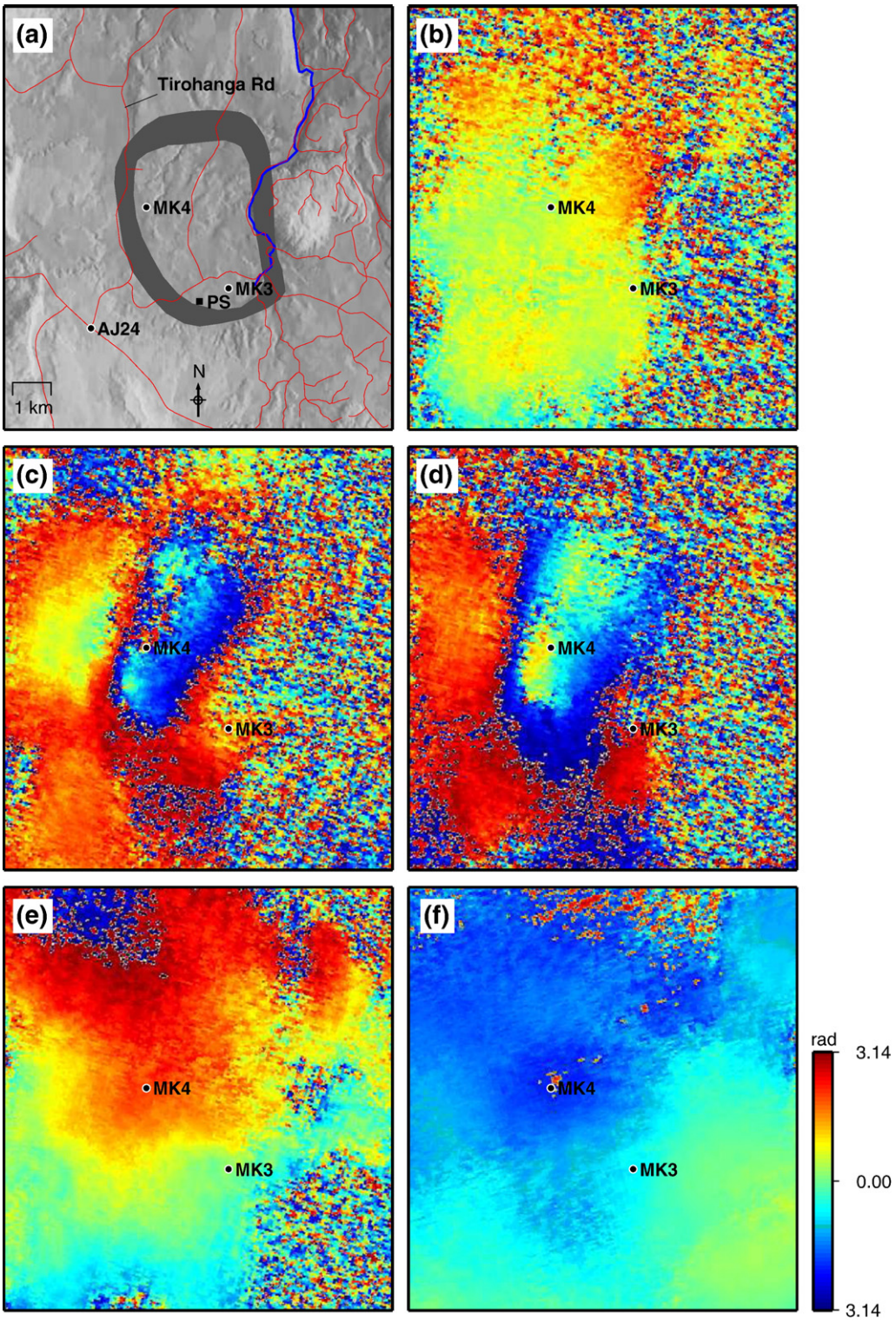

Fig. 10. (a) Location map of the Mokai geothermal field showing lakes and rivers (blue), road outlines (red), resistivity boundary (grey) (after Bibby et al., 1984), the Locations of the power station (PS) and selected benchmarks discussed in the text. Wrapped ERS interferograms of the Mokai geothermal field: (b) 05/03/1999–23/07/1999 (c) 10/12/1999–07/07/2000, (d) 14/01/2000–20/10/2000. (e) 02/06/2000–11/08/2000 (f) Wrapped Envisat interferogram 25/01/2004–13/06/2004. Red, yellow to blue represent increased distance to the satellite (i.e. apparent subsidence).

south, but not to the west, of the town. This is also apparent in the levelling data from 2001 to 2004 (Fig. 8d). Table 2 shows the change in deformation rate of the Taupo Fundamental benchmark (Taupo FM, Fig. 6), relative to benchmark A93, measured by levelling and InSAR.

A net uplift of Taupo airport cGPS station of about +25 mm, relative to Auckland GPS station, has also

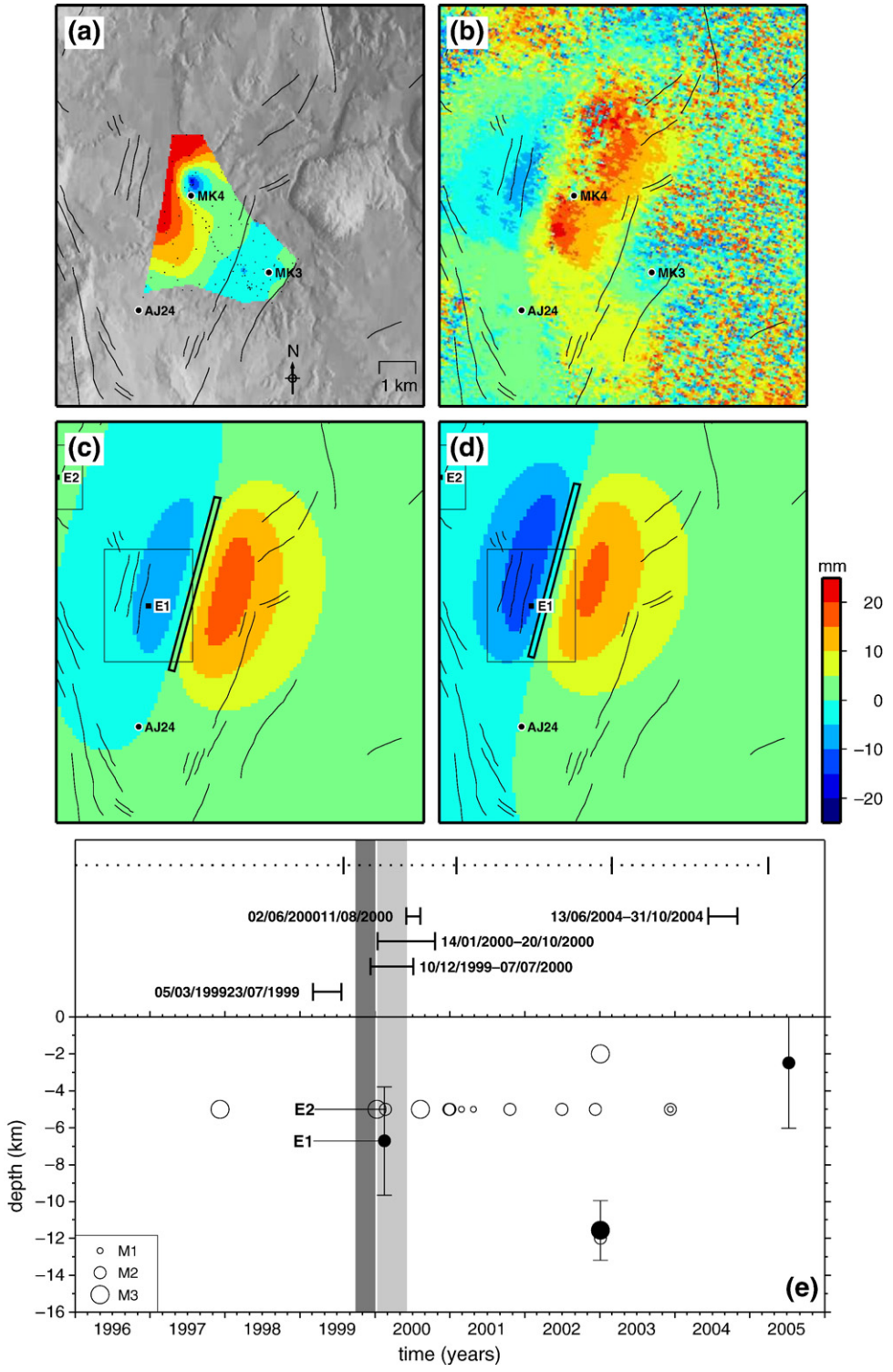

been measured by continuous GPS (Bromley, 2006). However, between 2002 and 2006, measured rates varied between −10 and +15 mm/year. Between 13/06/2004 and 31/10/2004, the period of the interferogram in Figs. 8b and 9, the 3-month running average (smoothed rates) suggests a rise of +1.85 mm (i.e. 3.6 mm/year).

Since the uplift is outside the boundary of the geothermal system it is probably not related to the geothermal subsidence. We cannot account for the cause of this uplift here without further modelling, which is beyond the scope of this paper. However, the area north of Lake Taupo has been known to undergo periods of episodic deformation (Grindley and Hull, 1986).

5.2.3. Mokai

The Mokai geothermal power plant was commissioned at the end of 1999 during the period of the ERS SAR acquisitions. The resistivity boundary of the geothermal systems and location of the power station are shown in Fig. 10a. The extraction is occurring in the area of well MK3. The Binary Turbine technology allows re-injection of the full discharge mass (liquid and steam) minus the non-condensible gases (about 1–3%). Well MK4 is one of the re-injection wells (For clarity other wells have not been marked).

Of the seventeen ERS interferograms that have coherent data in the Mokai area, the majority of them show no deformation (e.g. Fig. 10b); however, two independent interferograms from 1999 to 2000, both show an uplift signal (ground moves closer to the satellite) with similar size and shape coincident with the location of the Mokai geothermal field (Fig. 10c and d). Both of these interferograms overlap the period of commissioning of the 57 MW Mokai 1 power station between October 1999 and February 2000. The interferograms that precede this period (e.g. Fig. 10b) and one interferogram, 02/06/2000 to 11/08/2000 (10e) that overlaps the end of this period, do not show any uplift. Hence this signal must have occurred some time between 14/01/2000 and 02/06/2000. On 23/02/2000, a notable increase in thermal activity along a fault-controlled line of steaming craters adjacent to Tirohanga Road (west of MK4 in Fig. 10a) was observed. Over the following four years, this steam-dominated activity gradually cooled off. A relationship between this transient episode of increased thermal activity and movement on an underlying fault is conjectured.

The post-2003 Envisat data (e.g. Fig. 10f) show no evidence of any uplift at Mokai. The uplift in early 2000, about +20 mm at its maximum, has been identified in more than one independent interferogram and so is unlikely to be an atmospheric effect. We have also ruled out error during topographic phase removal by examining the satellite orbital geometry. Fig. 11a shows the deformation interpolated from levelling data from 1999 to 2001 (Energy Surveys Ltd, 2003), relative to benchmark AJ24. The uplift event of about +25 mm maximum is clearly visible. The levelling data from 2001 and 2003 (not shown) show no large scale subsidence signals, which suggests that the uplift that was observed between 1999 and 2001 was permanent.

Both Fig. 11a and unwrapped data from the 10/12/1999–07/07/2000 interferogram (Fig. 11b) show a smaller subsidence signal of about −5 mm/year in the area of deep fluid extraction (MK3). It is known that subsidence of up to −20 mm/year also occurred at Mokai between 1999 and 2005 but over a relatively small localised area coincident with the re-injection wells (near MK4). We suggest that this transient effect may be caused by initial contraction from cooling of reservoir rock caused by re-injection of cooler water at about 400 m depth. This subsidence event is visible in the 1999 to 2001 and 2001 to 2003 levelling data and also in a number of the Envisat interferograms (Fig. 10f) but not in any of the ERS interferograms.

The levelling data cover only a part of the interferogram. Fig. 11b shows that there is also a corresponding uplift and a small subsidence on the west side of the Tirohanga Road that is missed by the levelling. Simple modelling was carried out using the Range Change (RNGCHN) program of Feigl and Dupré (1999). The deformation pattern of Fig. 11b can be represented to first order by an eastward-dipping reverse fault motion (Fig. 11c) or a westward-dipping normal fault motion (Fig. 11d). The latter is more likely in this tectonic setting. The non-symmetric nature of the deformation pattern in the InSAR and the levelling along the length of the proposed fault rupture can be

Fig. 11. (a) Vertical displacement (in mm) obtained from levelling for the 08/1999 to 02/2001 period (Energy Surveys Ltd, 2003). The locations of levelling benchmarks used in the interpolation are shown. (b) Unwrapped interferogram 10/12/1999–07/07/2000 (c) Model A. (d) Model B. (e) Time and depth distribution of the earthquakes occurring in the area covered by Fig. 10. The filled circles represent those events where a depth range could be determined whereas the unfilled circles represent those events where the depth could only be restricted to depth shown. The circle diameter represents the magnitude rounded to the nearest integer. Also represented are the periods of the interferograms, discussed in the text and in Fig. 10, and the levelling periods. The dark grey shaded area represents the period of commissioning of the power station and the light grey shaded area represents the inferred time window of the uplift. Seismic events E1 and E2 discussed in the text are also labelled.

Table 3
Parameters used to model the deformation at the Mokai geothermal field caused by a single fault motion

Model	Description	Width	Length	Depth	Strike	Dip	U_1	U_3	U_3
		W	L	d					
		(km)	(km)	(km)	α (°)	δ (°)	(mm)	(mm)	(mm)
A	Eastward-dipping reverse	2	5	2	15	85	0	70	0
B	Westward-dipping normal	2	5	2	195	85	0	−85	0

explained by a small subsidence signal in the area of fluid extraction (near MK3) superimposed on the tectonic signal. The fault parameters of these two models are shown in Table 3. Fig. 11e shows that there were 20 recorded seismic events between 1996 and 2005 in the area defined by the extent of Fig. 10a. Most of these events had a local magnitude, M_L, of less than 3 and the depths are poorly constrained. Seismicity in this region typically occurs as swarms of events, making statistical analysis difficult, but there is no evidence of any significant changes in local seismic event rates following the Mokai power plant commissioning. However, two local earthquakes occurred during the period of the interferograms in Fig. 10c and d. The locations (with error bounds) are shown in Fig. 11c and d (E1, E2). Event E1, with M_L of 2.2, occurred on the 16/02/2000 in the region of one of the mapped faults in the area at a depth of about 7 km; event E2, with M_L of 2.4 occurred a few days later (22/02/2000) at a similar depth but 5 km to the north–west. However, events of this depth are probably of natural origin and not induced by the small pressure changes at about 400 m depth occurring at this time in the vicinity of the re-injection wells.

The earthquake models A and B have a slip-to-length ratio of 1.6×10^{-5}, which is outside the range of 1×10^{-4} to 2×10^{-5} defined by studying the relationships between source parameters from published InSAR studies (c.f. Funning, 2005). Also, models A and B have a seismic moment, M_0, of 2.5×10^{16} Nm, and a moment magnitude, M_w, of 4.8, calculated using the formula of Hanks and Kanamori (1979), which is significantly greater than that of E1. This suggests that most of the displacement on the fault may have occurred aseismically. Manville and Wilson (2003) suggest that historical vertical motions on the faults around northern Lake Taupo have appeared to consist of a period of aseismic uplift, seismic normal faulting, and a period of aseismic subsidence.

5.2.4. Rotorua

The Rotorua geothermal field is different from other fields considered in this study as it was not developed in a centralised/organised way. Since the 1920s, over 900 boreholes have been opened to provide heat and hot water for domestic, public and industrial use and thus it has the highest concentration of wells in the TVZ.

Levelling at Rotorua has not detected any subsidence due to aquifer compaction (B. Scott, personal communication, 2004); however, Hole et al. (2005c) identified subsidence signals from 1996 to 2000 in six interferograms of the urban area of Rotorua using ERS data. Fig. 12b shows a stack of two independent interferograms spanning a 2 year period from 1996 to 1998. There is an apparent subsidence signal of 8 mm/year (relative to point P, see Fig. 12a), coincident with the western edge of the geothermal area shown in Fig. 12a. This signal extends in a north–south direction and probably extends northwards although a lack of coherence in the park region means that this cannot be confirmed at present. It should be noted that areas of apparent uplift in the interferogram stack are coincident with areas of high relief, but the areas of subsidence do not appear to be correlated with topography. Analysis of Envisat data has not identified any further subsidence. We do not find any evidence to suggest an origin of this transient signal but it may relate to ground water movement associated with the contemporaneous level of the adjacent Lake Rotorua (B. Scott, personal communication, 2004).

6. Conclusions

Using a number of C-band interferograms we have mapped deformation at five of the geothermal systems of the TVZ that have undergone development. Subsidence signals have been identified at Ohaaki from 1999 to 2004, at Wairakei–Tauhara geothermal fields from 1996 to 2005, and at Rotorua from 1996 to 1998. A possible weak subsidence signal may be present at Rotokawa in 1999 and 2004, but this cannot be confirmed due to decorrelation in many of the long-term interferograms.

We have shown that the deformation field measured by InSAR is comparable with the results of precise levelling in areas where the phase gradients are low and we have contributed to knowledge of the subsidence

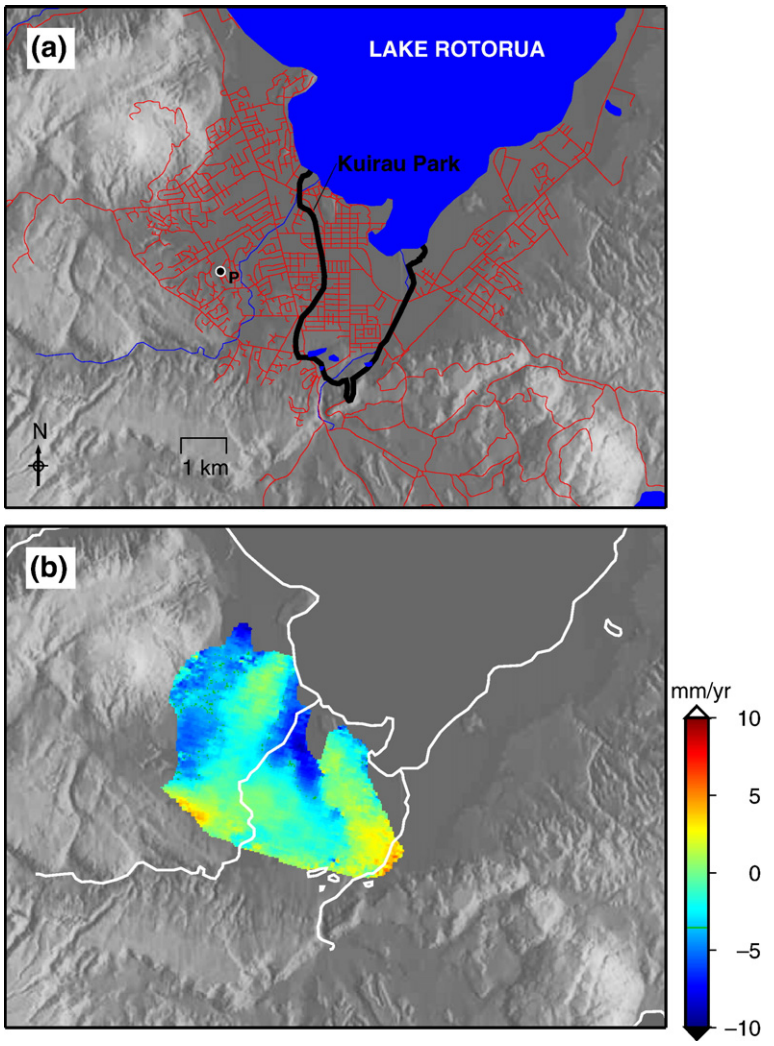

Fig. 12. (a) Location map of the Rotorua geothermal field showing lakes and rivers (blue), road outlines (red) and the boundary of the geothermal field determined by surface activity and drilling (Wood, 1992). (b) ERS stack of independent interferograms 12/05/1996–09/01/1999 and 24/05/1996–20/03/1998 showing line-of-sight displacement in mm/year.

behaviour at the edges of the fields away from the main subsidence areas where levelling benchmarks are not present or are sparse, such as parts of the Wairakei–Tauhara system.

As the InSAR measurements occur beyond the boundaries of the geothermal systems and beyond the scope of the levelling benchmarks, it is possible to interpret the subsidence signals in the context of the wider more regional deformation. At Wairakei, we have shown that the uplift measured in Taupo town from June to October 2004 seems to be focused only on Taupo town and the area to the south-west. Also, deformation measured at Mokai geothermal field using ERS InSAR from 1999 to 2000 has characterised an uplift event as probable fault motion, mostly aseismic but coinciding with the commencement of development, and with the observation of increased steam activity.

Although we have made successful measurements using InSAR, we acknowledge that the C-band InSAR technique has a number of limitations for geothermal subsidence mapping in the TVZ. At some of the geothermal areas in the TVZ, the gradient of the subsidence rate varies enormously across the subsiding area. Gradients are generally low across much of the field and then increase rapidly towards the centre of localised subsidence bowls. This presents conflicting

demands on the technique. Interferograms of more than 70 days are required in order to be able to measure the lesser deformation of the wider field above the noise and the atmospheric signals (although we have shown that stacking of 70-day pairs can give valuable results). However, the TVZ has extensive vegetative cover and increasing the time period of the interferograms beyond 70 days increases the temporal decorrelation in non-urban areas. In the TVZ, interferograms with a temporal separation greater than six to eight months are typically not useable whereas in arid areas, such as at the Coso geothermal area, longer term pairs (up to six years) can be used (Fialko and Simons, 2000) as the temporal decorrelation is less severe. Also, using SAR pairs with longer temporal separations reduces the ability of the technique to measure high deformation rate gradients, meaning additional processing of SAR pairs separated by shorter periods of time. The increasing number of Envisat images should improve the chances of a good Persistent Scatterer study (e.g. Ferretti et al., 2000, 2001; Hooper et al., 2004) which will enable DEM, orbital and atmospheric errors to be removed from each interferogram, utilising all SAR images and enabling a time series of deformation to be produced.

We have found that high data spatial filtering (4×16 looks) tends to underestimate the deformation rates in the centre of the subsidence bowls where deformation gradients are high and reduces the ability to resolve localised signals, such as at Crown Road in Taupo (Fig. 8d). Reducing the data spatial filtering increases the maximum detectable deformation gradient but reduces the coherence to such an extent that the Ohaaki, Mokai, Rotokawa and a large proportion of the Wairakei–Tauhara and Rotorua fields are only coherent in one or two interferograms. There is therefore a trade-off between coverage across the field and resolution of the measured deformation.

Although InSAR has provided valuable insights into the deformation of geothermal fields in the TVZ, the results are presently too sporadic for operational use and can only provide snapshots of the deformation of the TVZ when conditions are favourable. Regular monitoring of the fields is difficult as the number of suitable interferograms is likely to be small and it is not possible to predict in advance whether or not an image pair will be suitable; an InSAR satellite designed for ground motion movement would be required for this task (Stevens and Wadge, 2004), preferably with an L-band wavelength. The increased performance of L-band in the TVZ using JERS-1 data has been demonstrated by Hole et al. (2005a).

Acknowledgements

J. Hole acknowledges NERC studentship NER/S/A/2003/11319. Thanks to the New Zealand Foundation for Research and in Science and Technology (FRST) for covering some of the data and fieldwork costs under the PLT programme, and to the European Space agency for provision of the ERS SLC data under projects AO3-332 and Envisat data under AOE-1145. The additional RAW scenes were purchased under a Eurimage Research Club contract. Thanks also to the New Zealand Ministry of Agriculture and Forestry for providing the land cover (LCDB) data. The seismicity data are from the GEONET online catalogue (GeoNET, 2006b). The levelling data were provided by Steve Currie of Energy Surveys, New Zealand. Many of the figures were prepared using GMT software (Wessel and Smith, 1991).

References

Allis, R.G., 1997. The natural state and response to development of Kawerau geothermal field, New Zealand. Transactions of the Geothermal Resources Council 21, 3–10.

Allis, R.G., 2000. Review of subsidence at Wairakei field, New Zealand. Geothermics 29 (4–5), 455–478.

Allis, R.G., Lumb, J.T., 1992. The Rotorua geothermal field, New Zealand: its physical setting, hydrology, and response to exploitation. Geothermics 21 (1–2), 7–24.

Allis, R.G., Zhan, X., 2000. Predicting subsidence at Wairakei and Ohaaki geothermal fields, New Zealand. Geothermics 29 (4–5), 455–478.

Allis, R.G., Carey, B., Darby, D., Read, S.A.L., Rosenburg, M., Wood, C.P., 1997a. Subsidence at Ohaaki field, New Zealand. Proceedings of the 19th New Zealand Geothermal Workshop. Auckland, New Zealand, pp. 9–15.

Allis, R.G., Zhan, X., Carey, B., 1997b. Modelling of subsidence at Wairakei and Ohaaki fields. Proceedings of the 19th New Zealand Geothermal Workshop. Auckland, New Zealand, pp. 17–23.

Baran, I., Stewart, M., Claessens, S., 2005. A new functional model for determining minimum and maximum detectable deformation gradient resolved by satellite radar interferometry. IEEE Transactions on Geoscience and Remote Sensing 43 (4), 675–682.

Barringer, J.R.F., Lilburne, L., 1997. An evaluation of digital elevation models for upgrading New Zealand land resource inventory slope data. Proceedings of the 2nd Annual Conference of Geocomputation. Dunedin, New Zealand, pp. 109–116.

Beavan, J., Haines, J., 2001. Contemporary horizontal velocity and strain rate fields of the Pacific-Australian plate boundary zone through New Zealand. Journal of Geophysical Research 106 (B1), 741–770.

Bibby, H.M., Dawson, G.B., Rayner, H.H., Stagpoole, V.M., Graham, D.J., 1984. The structure of the Mokai geothermal-field based on geophysical observations. Journal of Volcanology and Geothermal Research 20 (1–2), 1–20.

Bibby, H.M., Caldwell, T.G., Davey, F.J., Webb, T.H., 1995. Geophysical evidence on the structure of the Taupo Volcanic Zone and its hydrothermal circulation. Journal of Volcanology and Geothermal Research 68 (1–3), 29–58.

Bromley, C.J., 2006. Predicting subsidence in New Zealand geothermal fields: a novel approach. Transactions of the Geothermal Resources Council 30, 142.

Bromley, C.J., Currie, S.A., 2003. Analysis of subsidence at Crown Road, Taupo: a consequence of declining groundwater. Proceedings of the 25th New Zealand Geothermal Workshop. Taupo, New Zealand.

Bromley, C.J., Hunt, T.M., Sherburn, S., Wood, C.P., 2000. Wairakei geothermal resource: geoscientific information, may 2000. technical report for Contact Energy, attached to applications for resource consents and assessment of environmental effects, Wairakei geothermal field. Lodged with Waikato Regional Council.

Carey, B., 2000. Wairakei 40 plus years of generation. Proceedings of the World Geothermal Congress. Kyushu-Tohoku, Japan.

Carnec, C., Fabriol, H., 1999. Monitoring and modeling land subsidence at Cerro Prieto geothermal field, Baja California, Mexico, using SAR interferometry. Geophysical Research Letters 26 (9), 1211–1214.

Central Surveys Ltd, 2002. Ohaaki levelling survey. Unpublished report for Contact Energy Ltd.

Closa, J., 1998. The influence of orbit precision in the quality of ERS SAR interferometric data. Tech. Rep. ES-TN-APP-APM-JC01, ESA.

Darby, D.J., Hodgkinson, K.M., Blick, G.H., 2000. Geodetic measurement of deformation in the Taupo Volcanic Zone, New Zealand: the north Taupo network revisited. New Zealand Journal of Geology and Geophysics 43 (2), 157–170.

Dunstall, M.G., 2005. 2000–2005 New Zealand country update. Proceedings of the World Geothermal Congress. Antalya, Turkey.

Energy Surveys Ltd, 2002. Rotokawa geothermal field: subsidence monitoring survey, March 2002. Unpublished report for Century Resources.

Energy Surveys Ltd, 2003. Mokai geothermal field subsidence monitoring survey, March 2003. Unpublished report for Tuaropaki Power Company.

Energy Surveys Ltd, 2005. Wairakei & Tauhara precise levelling and horizontal survey, September 2005. Unpublished report for Contact Energy Ltd.

Feigl, K., Dupré, E., 1999. RNGCHN: a program to calculate displacement components from dislocations in an elastic half-space with applications for modeling geodetic measurements of crustal deformation. Computers and Geosciences 25, 695–704.

Ferretti, A., Prati, C., Rocca, F., 2000. Nonlinear subsidence rate estimation using permanent scatterers in differential SAR interferometry. IEEE Transactions on Geoscience and Remote Sensing 38 (5), 2202–2212.

Ferretti, A., Prati, C., Rocca, F., 2001. Permanent scatterers in SAR interferometry. IEEE Transactions on Geoscience and Remote Sensing 39 (1), 8–20.

Fialko, Y., Simons, M., 2000. Deformation and seismicity in the Coso geothermal area, Inyo County, California: observations and modeling using satellite radar interferometry. Journal of Geophysical Research 105 (B9), 21781–21794.

Funning, G. J., 2005. Source parameters of large shallow earthquakes in the Alpine-Himalayan belt from InSAR and waveform modelling. Ph.D. thesis, University of Oxford.

GeoNET, 2006a. New Zealand active faults database. Online database. URL http://data.gns.cri.nz/af/(accessed 18 June 2006).

GeoNET, 2006b. New Zealand earthquake hypocentre locations. Online database. URL http://data.geonet.org.nz/QuakeSearch/index.jsp (accessed 16 March 2006).

Ghiglia, D., Pritt, M.D., 1998. Two-dimensional Phase Unwrapping: Theory, Algorithms and Software. Wiley Interscience, New York.

Glover, R.B., Hunt, T.M., Severne, C.M., 2000. Impacts of development on a natural thermal feature and their mitigation — Ohaaki Pool, New Zealand. Geothermics 29 (4–5), 509–523.

Goldstein, R.M., Werner, C.L., 1998. Radar interferogram filtering for geophysical applications. Geophysical Research Letters 25 (21), 4035–4038.

Grindley, G.W., Hull, A.G., 1986. Historical Taupo earthquakes and earth deformation. Bulletin of the Royal Society of New Zealand 24, 173–186.

Hanks, T.C., Kanamori, H., 1979. Seismic moments of the larger earthquakes of the southern Californian region. Bulletin of the Geological Society of America 86, 1131–1139.

Hanssen, R.F., 2001. Radar Interferometry: data interpretation and analysis. Vol. 2 of Remote Sensing and Digital Image Processing. Kluwer Academic, Dordrecht, The Netherlands.

Helm, D.C., 1984. Reviews in Engineering Geology. Geological Society of America, Ch. Field based computation techniques for predicting subsidence due to fluid withdrawal, vol. VI.

Hochstein, M.P., 1995. Crustal heat transfer in the Taupo Volcanic Zone (New Zealand): comparison with other volcanic arcs and explanatory heat source models. Journal of Volcanology and Geothermal Research 68 (1–3), 117–151.

Hole, J.K., Hooper, A., Wadge, G., Stevens, N.F., 2005a. Measuring contemporary deformation in the Taupo volcanic zone, New Zealand using SAR interferometry. Proceedings of the FRINGE 2005 Workshop, Frascati, Italy. Frascati, Italy (CD-ROM).

Hole, J.K., Stevens, N.F., Bromley, C., Wadge, G., 2005b. Subsidence at the Wairakei–Tauhara geothermal field, New Zealand from 1996–2003 measured by ERS interferometry. Proceedings of the Annual Conference of the Remote Sensing and Photogrammetry Society (RSPSoc). Portsmouth, UK (CD-ROM).

Hole, J.K., Stevens, N.F., Wadge, G., 2005c. Surface deformation at Rotorua, New Zealand, measured by ERS InSAR, 1996–2003. Proceedings of the 2004 Envisat and ERS Symposium, vol. SP-572. Salzburg, Austria (CD-ROM).

Hooper, A., Zebker, H.A., Segall, P., Kampes, B.M., 2004. A new method for measuring deformation on volcanoes and other natural terrains using InSAR persistant scatterers. Geophysical Research Letters 31, L23611.

Kissling, W.M., Weir, G.J., 2005. The spatial distribution of the geothermal fields in the Taupo Volcanic Zone, New Zealand. Journal of Volcanology and Geothermal Research 145 (1–2), 136–150.

Land Information New Zealand, 1987. 1:50,000 topographic map Wairakei, Edition 1, 260-U17.

Manville, V., Wilson, C.J.N., 2003. Interactions between volcanism, rifting and subsidence: implications of intracaldera palaeoshorelines at Taupo volcano, New Zealand. Journal of the Geological Society 160 (1), 3–6.

Massonnet, D., Feigl, K.L., 1998. Radar interferometry and its application to changes in the earth's surface. Reviews of Geophysics 36 (4), 441–500.

Massonnet, D., Vadon, H., Rossi, M., 1996. Reduction of the need for phase unwrapping in radar interferometry. IEEE Transactions on Geoscience and Remote Sensing 34 (2), 489–497.

Massonnet, D., Holzer, T., Vadon, H., 1997. Land subsidence caused by the East Mesa geothermal field, California, observed by SAR interferometry. Geophysical Research Letters 24 (8), 901–904.

Risk, G.F., Bibby, H.M., Caldwell, T.G., 1999. Resistivity structure of the central Taupo Volcanic Zone, New Zealand. Journal of Volcanology and Geothermal Research 90, 163–181.

Rowland, J.V., Sibson, R.H., 2001. Extensional fault kinematics within the Taupo Volcanic Zone, New Zealand: soft-linked segmentation

of a continental rift system. New Zealand Journal of Geology and Geophysics 44 (2), 271–283.

Rowland, J.V., Sibson, R.H., 2004. Structural controls on hydrothermal flow in a segmented rift system, Taupo Volcanic Zone, New Zealand. Geofluids 4, 259–283.

Scott, B.J., Cody, A.D., 2000. Response of the Rotorua geothermal system to exploitation and varying management regimes. Geothermics 29 (4–5), 573–592.

Scott, B.J., Gordon, D.A., Cody, A.D., 2005. Recovery of Rotorua geothermal field, New Zealand: Progress, issues and consequences. Geothermics 34 (2), 159–183.

Soengkono, S., 1999. Te Kopia geothermal system (New Zealand) — the relationship between its structure and extent. Geothermics 28, 767–784.

Soengkono, S., 2000. Assessment of faults and fractures at the Mokai geothermal field. Proceedings of the World Geothermal Congress, WGC2000, Kyushu-Tohuku, Japan. Hyushu-Tohoku, Japan.

Stern, T., Benson, A., Stratford, W., Bannister, S., 2005. Rocks beneath New Zealand's Central North Island: mantle or crust? EOS Transactions of the American Geophysical Union 538.

Stevens, N.F., Wadge, G., 2004. Towards operational repeat pass SAR interferometry at active volcanoes. Natural Hazards 33, 46–76.

Stratford, W.R., Stern, T.A., 2004. Strong seismic reflections and melts in the mantle of a continental back-arc basin. Geophysical Research Letters 31, L0622.

Turner, G.J., 1985. Geothermal exploitation and the decline of the Rotorua geothermal field, Rotorua, New Zealand. Geophysical Research Letters 12 (1), 21–24.

Vasco, D.W., Wicks, C.W., Karasaki, K., Marques, O., 2002. Geodetic imaging: reservoir monitoring using satellite interferometry. Geophysical Journal International 149 (3), 555–571.

Wessel, P., Smith, W.H.F., 1991. Free software helps map and display data. EOS Transaction of the American Geophysical Union 72, 441.

White, P.J., 2005. Latest developments in subsidence at Wairakei–Tauhara. Programme and Abstracts, 27th New Zealand Geothermal Workshop. Rotorua, New Zealand.

Wilson, C.J.N., Houghton, B.F., McWilliams, M.O., Lanphere, M.A., Weaver, S.D., Briggs, R.M., 1995. Volcanic and structural evolution of the Taupo Volcanic Zone, New Zealand: a review. Journal of Volcanology and Geothermal Research 68 (1–3), 1–28.

Wood, C.P., 1992. Geology of the Rotorua geothermal system. Geothermics 21 (1–2), 25–41.

Wood, C.P., Brathwaite, R.L., Rosenberg, M.D., 2001. Basement structure, lithology and permeability at Kawerau and Ohaaki geothermal fields, New Zealand. Geothermics 30, 461–481.

Zebker, H.A., Villasenor, J., 1992. Decorrelation in interferometric radar echoes. IEEE Transactions on Geoscience and Remote Sensing 30 (5), 950–959.